Defining feasible bounds on muscle activation in a redundant biomechanical task: practical implications of redundancy

M.Hongchul Sohn [a], J. Lucas McKay [b], Lena H. Ting [a,b],*

[a] The George W. Woodruff School of Mechanical Engineering, Georgia Institute of Technology, GA, USA
[b] The Wallace H. Coulter Department of Biomedical Engineering, Georgia Institute of Technology and Emory University, GA, USA

ARTICLE INFO

ABSTRACT

Measured muscle activation patterns often vary significantly from musculoskeletal model predictions that use optimization to resolve redundancy. Although experimental muscle activity exhibits both inter- and intra-subject variability we lack adequate tools to quantify the biomechanical latitude that the nervous system has when selecting muscle activation patterns. Here, we identified feasible ranges of individual muscle activity during force production in a musculoskeletal model to quantify the degree to which biomechanical redundancy allows for variability in muscle activation patterns. In a detailed cat hindlimb model matched to the posture of three cats, we identified the lower and upper bounds on muscle activity in each of 31 muscles during static endpoint force production across different force directions and magnitudes. Feasible ranges of muscle activation were relatively unconstrained across force magnitudes such that only a few (0–13%) muscles were found to be truly "necessary" (e.g. exhibited non-zero lower bounds) at physiological force ranges. Most of the muscles were "optional", having zero lower bounds, and frequently had "maximal" upper bounds as well. Moreover, "optional" muscles were never selected by optimization methods that either minimized muscle stress, or that scaled the pattern required for maximum force generation. Therefore, biomechanical constraints were generally insufficient to restrict or specify muscle activation levels for producing a force in a given direction, and many muscle patterns exist that could deviate substantially from one another but still achieve the task. Our approach could be extended to identify the feasible limits of variability in muscle activation patterns in dynamic tasks such as walking.

© 2013 Elsevier Ltd. All rights reserved.

1. Introduction

Musculoskeletal redundancy (Bernstein, 1967) in biomechanical models is often addressed through optimizations that identify a unique muscle activation pattern among many possible. One popular criterion is minimizing muscle stress (Crowninshield and Brand, 1981) which has been widely applied to predict muscle coordination in simulations (Anderson and Pandy, 2001; Thelen et al., 2003; Erdemir et al., 2007). However, measured muscle activity often varies significantly from these predictions (Buchanan and Shreeve, 1996; Herzog and Leonard, 1991; Thelen and Anderson, 2006; van der Krogt et al., 2012). We currently lack methods for analyzing high-dimensional musculoskeletal models that would allow us to quantify the degree to which muscle activity may feasibly vary for a given motor task.

The first step to understand the variability in muscle activity with respect to musculoskeletal redundancy is to identify absolute biomechanical constraints on muscle activity for a given task. In contrast to optimization, this approach seeks to find the full range of possible solution sets available to the nervous system (Kutch and Valero-Cuevas, 2011). In particular, identifying the explicit bounds on muscle activation can reveal whether predicted or measured muscle activity is due to biomechanical requirements necessary to perform the task, or because of allowable variability in how the task can be achieved. Identifying feasible bounds of muscle activity can also describe the degree to which muscle activity may deviate from optimal solutions.

This study was motivated by experimentally-observed inter- and intra-subject variability during reactive balance control (Horak and Nashner, 1986; Torres-Oviedo et al., 2006; Torres-Oviedo and Ting, 2007). For example in cats, when producing an extensor force vector (Fig. 1A, F_{EXT}), knee extensor *vastus medialis* (VM) was recruited consistently across animals, but hip and knee flexor *medial sartorius* (SARTm) was recruited at different levels across animals (Fig. 1B, F_{EXT}). Conversely, when producing a flexor force vector (Fig. 1A, F_{FLEX}), VM recruitment varied across animals but SARTm was recruited consistently in all animals (Fig. 1B, F_{FLEX}).

Here, we identified feasible ranges of muscle activation during static force production in a detailed model of the cat hindlimb

* Corresponding author at: Department of Biomedical Engineering, Georgia Institute of Technology and Emory University, 313 Ferst Drive, Atlanta, GA 30332-0535. Tel.: +1 404 894 5216.
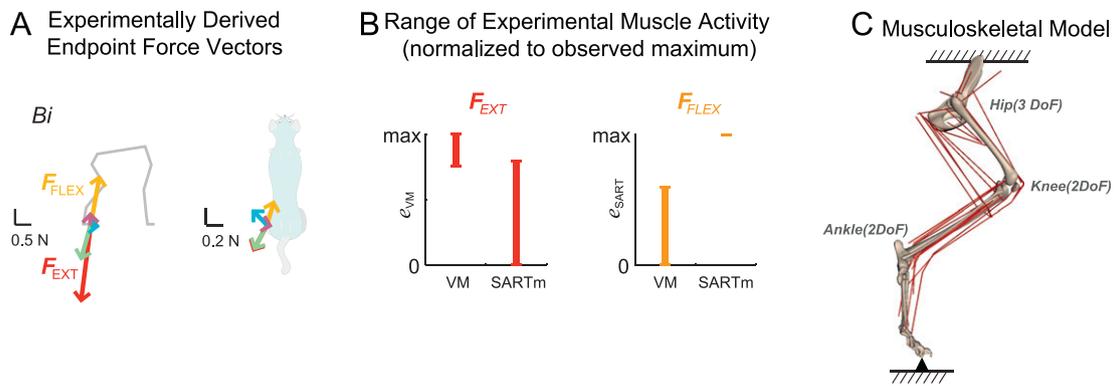E-mail addresses: lting@emory.edu, lena.ting@bme.gatech.edu (L.H. Ting).

Fig. 1. (A) Experimentally-measured hindlimb endpoint force vectors in cat *Bi* from Torres-Oviedo et al. (2006). Extensor force vector (F_{EXT}, red) and flexor force vectors (F_{FLEX}, yellow) were essentially identical across cats. (B) Range of experimental muscle activity for producing F_{EXT} and F_{FLEX} across 3 cats. When producing F_{EXT}, VM was consistently activated in all animals, whereas the activation level of SARTm varied across animals. For F_{FLEX}, SARTm was activated consistently in all animals and VM was activated at varying levels across animals. (C) Musculoskeletal model of the cat hindlimb (Burkholder and Nichols, 2004) with seven rotational degrees of freedom (3 at the hip, 2 each at the knee and ankle) and 31 muscles. In this static model, the pelvis was fixed to the ground and the endpoint, defined at the MTP joint, was connected to the ground via gimbal joint where moments were constrained to be zero.

(Fig. 1C; Burkholder and Nichols, 2004; McKay and Ting, 2008). We identified the upper and lower bounds on muscle activity in each of 31 muscles during endpoint force production in different directions and magnitudes. Muscles with non-zero lower bounds were classified as "necessary", whereas muscles with zero lower bounds were classified as "optional". Muscles were further classified to have "sub-maximal upper bound" or "maximal upper bound". To examine the degree to which feasible muscle activation patterns could deviate from an optimal solution, we compared these bounds to muscle activation patterns predicted by minimizing muscle stress (Crowninshield and Brand, 1981), or scaling the pattern required for maximum force generation (Valero-Cuevas, 2000).

2. Methods

2.1. Musculoskeletal model

The static three-dimensional musculoskeletal model of the cat hindlimb (Burkholder and Nichols, 2004) included seven rotational degrees of freedom (Fig. 1C). 31 muscles (Table 1) produced net joint torque $\vec{\tau}$ (7 × 1), and a resulting endpoint wrench (force and moment vector) $\vec{F}_{End}$ (6 × 1) at the metatarsophalangeal (MTP) joint. The MTP was connected to the ground via a gimbal joint (Fig. 1C), representing the experimental condition of a freely standing cat where the foot never lost contact or slipped with respect to the ground (Jacobs and Macpherson, 1996). Endpoint moments were constrained to be zero, a conservative approximation of the small moments that can be supported by the contact area of cat's foot (McKay et al., 2007). The model defined the mapping from muscle activation vector $\vec{e}$ (31 × 1) to endpoint wrench $\vec{F}_{End}$:

$$RF_{AFL}\vec{e} = \vec{\tau} = J^T\vec{F}_{End}, \qquad (1)$$

where J is a geometric Jacobian (6 × 7), R is a moment arm matrix (7 × 31) that maps muscle forces to joint torques, and F_{AFL} is a diagonal matrix (31 × 31) of scaling factors based on the active force–length property of muscle (Zajac, 1989). To approximate the operating region on the force–length relationship curve commonly observed in habitual postures, all muscles were set to 95% optimal fiber length (Burkholder and Lieber, 2001; Roy et al., 1997; Sacks and Roy, 1982). We found matrices J and R for each of 3 cats Bi, Ni, and Ru based on their average kinematic configuration measured during quiet standing (McKay et al., 2007) using Neuromechanic software (Bunderson et al., 2012).

2.2. Target endpoint forces

Five experimentally-derived force vectors in each cat measured during postural responses to translational support perturbation (Torres-Oviedo et al., 2006) were used as target endpoint force vector directions (Fig. 1A). These force vectors represented the active response of the cats following perturbation, measured as the change in the ground reaction force from the background level, averaged over the postural response period 150–200 ms following the perturbation (Jacobs and Macpherson, 1996), where only small angular deviations in joint angles ($\leq 2°$) are

Table 1
Muscles included in the hindlimb model and abbreviations.

Name	Abbreviation	Name	Abbreviation
Adductor femoris	ADF	*Plantaris*	PLAN
Adductor longus	ADL	*Iliopsoas*	PSOAS
Biceps femoris anterior	BFA	*Peroneus tertius*	PT
Biceps femoris posterior	BFP	*Pyriformis*	PYR
Extensor digitorum longus	EDL	*Quadratus femoris*	QF
Flexor digitorum longus	FDL	*Rectus femoris*	RF
Flexor hallucis longus	FHL	*Sartorius*	SART
Gluteus maximus	GMAX	*Semimembranossus*	SM
Gluteus medius	GMED	*Soleus*	SOL
Gluteus minimus	GMIN	*Semitendinosus*	ST
Gracilis	GRAC	*Tibialis anterior*	TA
Lateral gastrocnemius	LG	*Tibialis posterior*	TP
Medial gastrocnemius	MG	*Vastus intermedius*	VI
Peroneus brevis	PB	*Vastus lateralis*	VL
Pectineus	PEC	*Vastus medialis*	VM
Peroneus longus	PL		

observed (Ting and Macpherson, 2004). To examine biomechanical constraints across force magnitudes, we scaled each force vector from 0 to the maximum feasible level that could be produced by the model, identified using linear programming. We found the muscle activation pattern $\vec{e}^{MAX}$ that maximized force magnitude:

$$\vec{e}^{MAX}: \text{Find } \vec{e} \text{ s.t. } \|(RF_{AFL}\vec{e})\cdot(J^T\vec{F}_{Exp})\| \text{ is maximized, while } (RF_{AFL}\vec{e}) \times (J^T\vec{F}_{Exp}) = 0, \qquad (2)$$

where the cross product constraint in Eq. (2) ensured the preservation of force direction. Activation of each muscle was constrained between 0 and 1, and endpoint moments were constrained to be zero. The maximum feasible force in direction of the experimental force vector is given by:

$$\vec{F}^{MAX}_{EXP} = RF_{AFL}\frac{\vec{e}^{MAX}}{J^T\vec{F}_{Exp}}\vec{F}_{Exp}. \qquad (3)$$

2.3. Lower and upper bounds on muscle activation

We used linear programming to identify the lower bound (e_m^{LB}) and the upper bound (e_m^{UB}) on the feasible activation level of each muscle as the magnitude (α) of each of the target endpoint force vectors was scaled from 0 to 1 (Eqs. (4) and (5)). Grid spacing $\Delta\alpha = 0.1$ was used from $\alpha = 0.0$ to 0.9, and grid spacing $\Delta\alpha = 0.02$ from $\alpha = 0.9$ to 1.0 because initial tests revealed rapid changes for higher values of α. For each muscle and each value of α, the lower and upper bound was identified as follows:

$$e_m^{LB}: \text{Find } \vec{e} \text{ s.t. } |e_m| \text{ is minimized, while } RF_{AFL}\vec{e} = \alpha J^T\vec{F}^{MAX}_{Exp} \qquad (4)$$

$$e_m^{UB}: \text{Find s.t. } |e_m| \text{ is maximized, while } RF_{AFL}\vec{e} = \alpha J^T\vec{F}^{MAX}_{Exp} \qquad (5)$$

Each muscle was classified as *necessary* or *optional* based on whether, and at what force magnitude the muscle became biomechanically required to generate
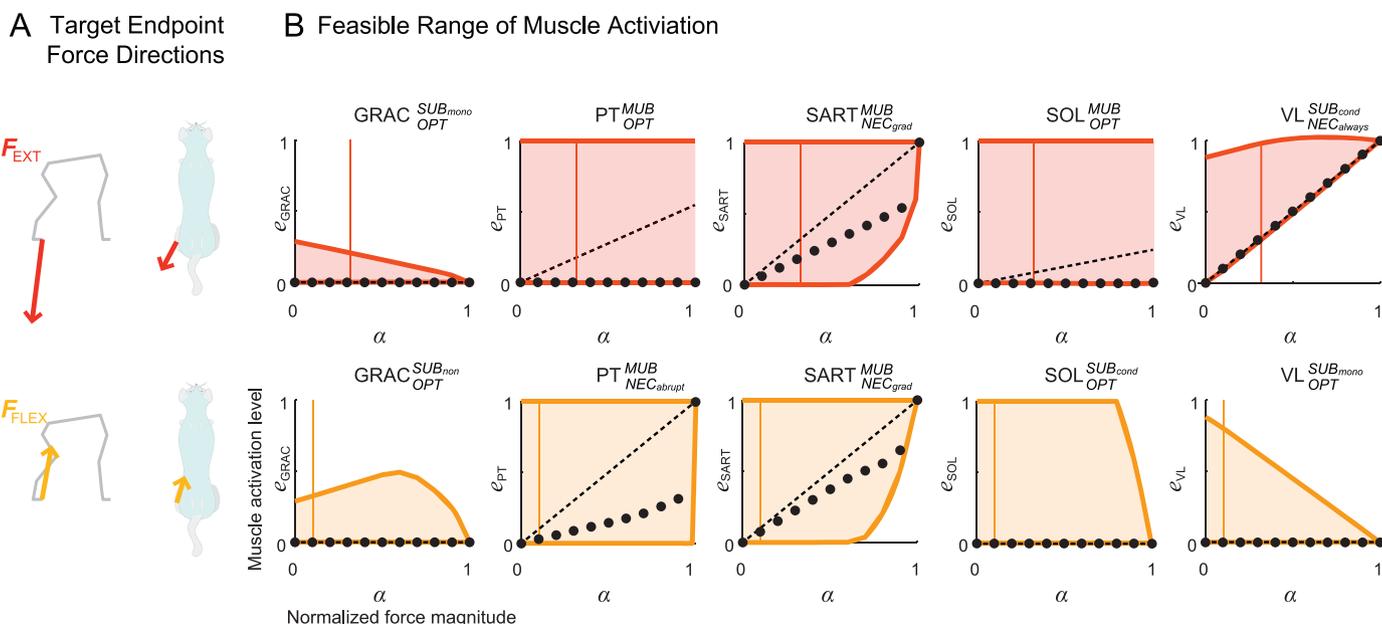
Fig. 2. (A) Two representative target endpoint force directions for cat *Bi*: F_{EXT} (red, top row) and F_{FLEX} (yellow, bottom row). (B) Identified feasible range of activation as a function of normalized force magnitude (α) for five muscles in cat *Bi*: GRAC, PT, SART, SOL and VL. Feasible range (shaded) is defined by the difference between the lower bound (e_m^{LB}, bottom trace) and the upper bound (e_m^{UB}, top trace). Muscles with zero lower bounds were categorized as optional (*OPT*), e.g. GRAC, PT, SOL for F_{EXT}, and GRAC, SOL, for F_{FLEX}. Muscles were categorized as necessary (*NEC*) if lower bounds were nonzero at any force level, and further subdivided into categories of becoming necessary gradually, e.g. SART for F_{EXT} and F_{FLEX}; only near maximal force, e.g. PT for F_{FLEX}; or always, e.g. VL for F_{EXT}. Muscles were also classified as having maximal (*MUB*) upper bounds e.g. PT, SART, SOL for F_{EXT} and PT, SART, for F_{FLEX}; or having sub-maximal (*SUB*) upper bounds, either monotonically, e.g. GRAC for F_{EXT} and VL for F_{FLEX}; nonmonotonically, e.g. GRAC for F_{FLEX}; or conditionally, e.g. VL for F_{EXT} and SOL for F_{FLEX}. The vertical line indicates the experimental force levels at which most muscles had zero lower bound and were practically "optional"; of the muscles shown, only VL for F_{EXT} was truly "necessary". Feasible ranges were wide in general, where activity of a muscle could deviate substantially from the solutions predicted by either minimizing muscle stress (dots), or scaling the pattern required for maximal force (dashed lines). Note that neither strategy predicted the recruitment of optional muscles.

endpoint force, corresponding to a nonzero lower bound. Similarly, we classified muscles as having *sub-maximal upper bound* or *maximal upper bound* based on whether the upper bound was less than or equal to full activation. Considering all combinations of animals, muscles, bounds, endpoint force vectors, and levels of α resulted in 13,206 separate linear programming calls.

Lower and upper bounds identified at $\alpha=0$ were considered as a special case because they do not depend on direction of the endpoint force vector and reveal the feasible muscle activation patterns associated with zero net torque production, which we call the *physiological null space*.

2.4. Comparison to predicted solutions from suggested neural strategies

We compared the feasible range of individual muscle activity to solutions for muscle activation patterns identified by (1) minimizing muscular stress (Crowninshield and Brand, 1981) in the form of sum-squared muscle activation (Thelen et al., 2003) and (2) scaling the muscle activation pattern for the maximal task (Valero-Cuevas, 2000). For the minimum stress strategy, muscle patterns $\vec{e}^{\,min}$ were identified for each level of α via quadratic programming as follows:

$$\vec{e}^{\,Min}: \text{Find } \vec{e} \text{ s.t. } \sum_{m=1}^{31} e_m^2 \text{ is minimized, while } \mathbf{RF}_{AFL}\vec{e} = \alpha \mathbf{J}^T \vec{F}_{Exp}^{\,MAX} \quad (6)$$

For the scaling strategy, $\vec{e}^{\,MAX}$ identified in Eq. (2) was scaled proportional to α.

3. Results

3.1. Bounds on muscle activation during endpoint force production

The feasible range of muscle activity for each muscle changed non-uniformly as force magnitude α increased from zero to maximal in a given target endpoint force direction (e.g. Fig. 2B, shaded region). This range was defined by the difference between the lower bound (Fig. 2B, bottom trace) and upper bound (Fig. 2B, top trace) at a given α. In each animal, similar patterns of the feasible range of muscle activity was identified across muscles and force directions. Therefore, two force directions are used for

detailed illustration of the results: an extensor force F_{EXT} (Fig. 2A, red) and a flexor force F_{FLEX} (Fig. 2A, yellow).

Most muscles had zero lower bound for all force magnitudes ($e_m^{LB}=0$ for all α) and were classified as optional (*OPT*). Muscles for which lower bound became nonzero for some α were classified as necessary; they were either always necessary (*NEC$_{always}$*: $e_m^{LB}>0$ for all α), or became gradually necessary as α increased (*NEC$_{grad}$*: $e_m^{LB}>0$ at $0<c<\alpha<1$), or became necessary only at the maximum force level (*NEC$_{abrupt}$*: $e_m^{LB}>0$ only at $\alpha\approx1$). Across cats, $71\pm7\%$ of muscles were optional for the generation of F_{EXT}, and 58%—but not the same muscles—were optional for generation of F_{FLEX} (Table 2). For example, in cat *Bi* (Fig. 2B), GRAC, PT, SOL were *OPT* for F_{EXT}, and GRAC, SOL, VL were *OPT* for F_{FLEX}. VL was *NEC$_{always}$* for F_{EXT}, SART was *NEC$_{grad}$* for both F_{EXT} and F_{FLEX}, and PT was *NEC$_{abrupt}$* for F_{FLEX}.

Less than 1/3 of muscles had an upper bound of one for all force magnitudes and were classified as having maximal upper bound (*MUB*: $e_m^{UB}=1$ for all α). Muscles with upper bound less than one for some range of α were classified as having sub-maximal upper bound conditionally (*SUB$_{cond}$*: $e_m^{UB}<1$ for $0<\alpha<c$ or $c<\alpha<1$). Muscles for which the upper bound was always less than one were classified as having sub-maximal upper bound ($e_m^{UB}<1$ for all α), but were further categorized based on whether the upper bound changed monotonically (*SUB$_{mono}$*) or non-monotonically (*SUB$_{non}$*). Across cats, $32\pm3\%$ of the muscles had maximal upper bound for generating F_{EXT}, $22\pm2\%$ had sub-maximal upper bound for generating F_{FLEX} (Table 3). For example, PT, SART, SOL were *MUB* for F_{EXT}, and PT and SART were *MUB* for F_{FLEX} in cat *Bi* (Fig. 2B). VL was *SUB$_{cond}$* and GRAC was *SUB$_{mono}$* for F_{EXT}, whereas SOL was *SUB$_{cond}$*, VL was *SUB$_{mono}$*, and GRAC was *SUB$_{non}$* for F_{FLEX}.

Muscle classification in terms of the lower and upper bounds depended on the target endpoint force direction (Tables 2 and 3). In total, 20 muscles in *Bi*, 20 in *Ni*, 19 in *Ru*, showed different

Table 2
Muscle classification in terms of lower bound (e_m^{LB}) behavior.

	Bi		Ni		Ru	
	F_{EXT}	F_{FLEX}	F_{EXT}	F_{FLEX}	F_{EXT}	F_{FLEX}
ADF	*OPT*	*OPT*	*OPT*	*OPT*	*OPT*	*OPT*
ADL	*OPT*	*OPT*	*OPT*	*OPT*	*OPT*	*OPT*
BFA	*OPT*	*OPT*	*OPT*	*OPT*	*OPT*	*OPT*
BFP	*NEC_{always}*	*NEC_{grad}*	*NEC_{always}*	*NEC_{grad}*	*NEC_{grad}*	*NEC_{grad}*
EDL	***OPT***	***NEC_{grad}***	***OPT***	***NEC_{grad}***	***OPT***	***NEC_{grad}***
FDL	*OPT*	*OPT*	*OPT*	*OPT*	*OPT*	*OPT*
FHL	*OPT*	*OPT*	*OPT*	*OPT*	*OPT*	*OPT*
GMAX	*OPT*	*OPT*	*OPT*	*OPT*	*OPT*	*OPT*
GMED	*NEC_{abrupt}*	*NEC_{always}*	*NEC_{grad}*	*NEC_{grad}*	*NEC_{grad}*	*NEC_{grad}*
GMIN	*OPT*	*OPT*	*OPT*	*OPT*	*NEC_{abrupt}*	*NEC_{abrupt}*
GRAC	*OPT*	*OPT*	*OPT*	*OPT*	*OPT*	*OPT*
LG	***OPT***	***NEC_{grad}***	***OPT***	***NEC_{grad}***	***OPT***	***NEC_{grad}***
MG	***OPT***	***NEC_{abrupt}***	***OPT***	***NEC_{abrupt}***	*OPT*	*OPT*
PB	***OPT***	***NEC_{abrupt}***	***OPT***	***NEC_{grad}***	*OPT*	*OPT*
PEC	*OPT*	*OPT*	*OPT*	*OPT*	*OPT*	*OPT*
PL	***OPT***	***NEC_{abrupt}***	***OPT***	***NEC_{grad}***	***OPT***	***NEC_{abrupt}***
PLAN	*OPT*	*OPT*	*OPT*	*OPT*	*OPT*	*OPT*
PSOAS	*NEC_{grad}*	*NEC_{grad}*	*NEC_{grad}*	*NEC_{grad}*	*NEC_{grad}*	*NEC_{grad}*
PT	***OPT***	***NEC_{abrupt}***	***OPT***	***NEC_{abrupt}***	***OPT***	***NEC_{abrupt}***
PYR	*NEC_{grad}*	*NEC_{grad}*	*NEC_{grad}*	*NEC_{grad}*	*NEC_{grad}*	*NEC_{grad}*
QF	*NEC_{grad}*	*NEC_{grad}*	*NEC_{grad}*	*NEC_{grad}*	*NEC_{grad}*	*NEC_{grad}*
RF	*OPT*	*OPT*	*OPT*	*OPT*	***NEC_{grad}***	***OPT***
SART	*NEC_{grad}*	*NEC_{grad}*	*NEC_{grad}*	*NEC_{grad}*	*NEC_{grad}*	*NEC_{grad}*
SM	*OPT*	*OPT*	*OPT*	*OPT*	*OPT*	*OPT*
SOL	*OPT*	*OPT*	*OPT*	*OPT*	*OPT*	*OPT*
ST	*OPT*	*OPT*	*OPT*	*OPT*	***OPT***	***NEC_{abrupt}***
TA	*NEC_{abrupt}*	*NEC_{grad}*	***OPT***	***NEC_{grad}***	*NEC_{abrupt}*	*NEC_{grad}*
TP	*OPT*	*OPT*	*OPT*	*OPT*	*OPT*	*OPT*
VI	***NEC_{abrupt}***	***OPT***	*OPT*	*OPT*	***NEC_{grad}***	***OPT***
VL	***NEC_{always}***	***OPT***	***NEC_{always}***	***OPT***	***NEC_{grad}***	***OPT***
VM	*OPT*	*OPT*	*OPT*	*OPT*	*OPT*	*OPT*

OPT: e_m^{LB} is always zero; *NEC_{always}*: e_m^{LB} is always non-zero; *NEC_{grad}*: e_m^{LB} becomes non-zero gradually; *NEC_{abrupt}*: e_m^{LB} becomes non-zero abruptly at maximal force magnitude. Muscle that changed classifications of *necessary* versus *optional* across the two force directions are shown in bold.

Table 3
Muscle classification in terms of upper bound (e_m^{UB}) behavior.

	Bi		Ni		Ru	
	F_{EXT}	F_{FLEX}	F_{EXT}	F_{FLEX}	F_{EXT}	F_{FLEX}
ADF	*SUB_{mono}*	*SUB_{mono}*	*SUB_{mono}*	*SUB_{mono}*	*SUB_{mono}*	*SUB_{non}*
ADL	*SUB_{cond}*	*SUB_{cond}*	*SUB_{cond}*	*SUB_{cond}*	*SUB_{cond}*	*SUB_{cond}*
BFA	*SUB_{mono}*	*SUB_{mono}*	*SUB_{mono}*	*SUB_{non}*	*SUB_{mono}*	*SUB_{non}*
BFP	*SUB_{mono}*	*SUB_{mono}*	*SUB_{mono}*	*SUB_{mono}*	*SUB_{mono}*	*SUB_{mono}*
EDL	***SUB_{cond}***	***MUB***	*SUB_{cond}*	*SUB_{non}*	***SUB_{Cond}***	***MUB***
FDL	***MUB***	***SUB_{cond}***	***MUB***	***SUB_{cond}***	***MUB***	***SUB_{cond}***
FHL	*SUB_{cond}*	*SUB_{cond}*	*SUB_{cond}*	*SUB_{cond}*	*SUB_{cond}*	*SUB_{cond}*
GMAX	*SUB_{cond}*	*SUB_{cond}*	*SUB_{cond}*	*SUB_{cond}*	*SUB_{cond}*	*SUB_{cond}*
GMED	*SUB_{mono}*	*SUB_{mono}*	*SUB_{mono}*	*SUB_{non}*	*SUB_{mono}*	*SUB_{mono}*
GMIN	*SUB_{cond}*	*SUB_{cond}*	*SUB_{cond}*	*SUB_{cond}*	*MUB*	*MUB*
GRAC	*SUB_{mono}*	*SUB_{non}*	*SUB_{mono}*	*SUB_{non}*	*SUB_{mono}*	*SUB_{non}*
LG	*SUB_{mono}*	*SUB_{non}*	*SUB_{mono}*	*SUB_{non}*	*SUB_{mono}*	*SUB_{mono}*
MG	*SUB_{mono}*	*SUB_{non}*	*SUB_{mono}*	*SUB_{non}*	*SUB_{mono}*	*SUB_{mono}*
PB	***MUB***	***SUB_{cond}***	***MUB***	***SUB_{cond}***	***MUB***	***SUB_{cond}***
PEC	*SUB_{cond}*	*SUB_{cond}*	*SUB_{cond}*	*SUB_{cond}*	*SUB_{cond}*	*SUB_{cond}*
PL	*MUB*	*MUB*	*MUB*	*MUB*	***MUB***	***SUB_{cond}***
PLAN	*SUB_{mono}*	*SUB_{non}*	*SUB_{mono}*	*SUB_{non}*	*SUB_{mono}*	*SUB_{mono}*
PSOAS	*MUB*	*MUB*	*MUB*	*MUB*	*MUB*	*MUB*
PT	*MUB*	*MUB*	*MUB*	*MUB*	*MUB*	*MUB*
PYR	*MUB*	*MUB*	*MUB*	*MUB*	*MUB*	*MUB*
QF	*SUB_{cond}*	*SUB_{cond}*	***MUB***	***SUB_{cond}***	*SUB_{cond}*	*SUB_{cond}*
RF	*SUB_{mono}*	*SUB_{non}*	*SUB_{mono}*	*SUB_{non}*	*SUB_{cond}*	*SUB_{cond}*
SART	*MUB*	*MUB*	*MUB*	*MUB*	*MUB*	*MUB*
SM	*SUB_{mono}*	*SUB_{non}*	*SUB_{mono}*	*SUB_{non}*	*SUB_{non}*	*SUB_{non}*
SOL	***MUB***	***SUB_{cond}***	***MUB***	***SUB_{cond}***	***MUB***	***SUB_{cond}***
ST	*SUB_{mono}*	*SUB_{non}*	*SUB_{mono}*	*SUB_{non}*	*SUB_{non}*	*SUB_{non}*
TA	*MUB*	*MUB*	*MUB*	*MUB*	*MUB*	*MUB*
TP	*SUB_{mono}*	*SUB_{mono}*	*SUB_{mono}*	*SUB_{mono}*	*SUB_{mono}*	*SUB_{mono}*
VI	*SUB_{cond}*	*SUB_{cond}*	*SUB_{cond}*	*SUB_{cond}*	***MUB***	***SUB_{cond}***
VL	*SUB_{cond}*	*SUB_{mono}*	*SUB_{cond}*	*SUB_{mono}*	*SUB_{mono}*	*SUB_{mono}*
VM	*SUB_{mono}*	*SUB_{non}*	*SUB_{mono}*	*SUB_{non}*	*SUB_{cond}*	*SUB_{cond}*

MUB: e_m^{UB} is always one (maximal); *SUB_{cond}*: e_m^{UB} is sub-maximal only at certain range of α; *SUB_{mono}*: e_m^{UB} is always sub-maximal and changes monotonnically; *SUB_{non}*: e_m^{UB} is always sub-maximal and changes non-monotonically. Muscles that changed classification of *sub-maximal upper bound* versus *maximal upper bound* across the two force directions are shown in bold.

behavior for F_{FLEX} as compared to F_{EXT}. The classification of muscles was relatively consistent across cats for a given force direction: for the lower bound, only 3 muscles were categorized differently across all cats for both F_{EXT} and F_{FLEX}, and for the upper bound, only 4 muscle were categorized differently across 3 cats for both F_{EXT} and F_{FLEX} Because the direction of endpoint force vectors was very consistent ($\cos\theta > 0.998$) across cats for both F_{EXT} and F_{FLEX}, these differences in the categorization were due to differences in posture.

Regardless of classifications, the feasible range of muscle activity at physiological levels of force did not identify a clear pattern of muscle activity necessary to achieve the task. At experimentally-observed force magnitudes (Fig. 2B, vertical lines), lower bounds were often zero, suggesting that most muscles were optional at those force levels. Across animals, α_{exp} was 0.32, 0.77, and 0.19 in *Bi*, *Ni* and *Ru* respectively for F_{EXT} and 0.12, 0.11, 0.11 for F_{FLEX}.

3.2. Comparison of identified bounds and predictions of neural strategies

Because of the large feasible range, muscle activity could deviate substantially from two commonly suggested muscle coordination strategies. Both solutions fell within the feasible ranges of muscle activity, and typically near—but not necessarily at—the lower bound. Both the scaling strategies (Fig. 2B, dashed line) and the minimum stress strategy (Fig. 2B, dotted line) recruited necessary muscles at the earliest nonzero α even
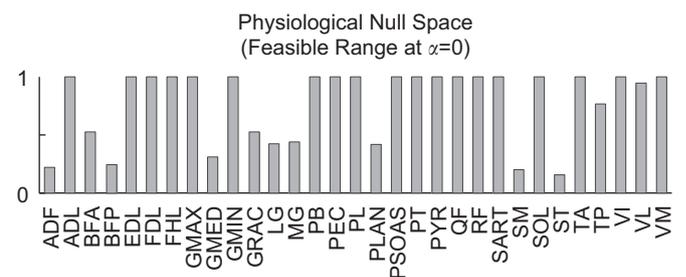

Fig. 3. Physiological null space, defined as the feasible range at $\alpha=0$ in cat *Ru*. While many muscles could be maximally activated, several muscles were limited in the maximum activation that would allow zero net torque production. Upper bounds of muscles that produce large torques (e.g. BFP) were typically limited because of the lower torque-generating capabilities of their antagonists.

though the lower bounds on feasible muscle activity were typically zero at low force magnitudes (e.g. Fig. 2B, SART). Optional muscles were never selected in either strategy (e.g. Fig. 2B, GRAC for F_{EXT} and VL for F_{FLEX}). Although the upper and lower bounds typically converged on a unique solution for maximum force production (Fig. 2B, bottom row), this was not always the case in ankle muscles for F_{EXT} (Fig. 2B, top row, PT and SOL), indicating that redundancy remained even at maximum force magnitudes. This resulted from low ankle torque (~ 0.004 N m) compared to knee torque (~ 0.5 N m) required to produce F_{EXT}.

3.3. Physiological null space at $\alpha = 0$

Approximately 1/3 of muscles had upper bounds of less than one for zero net torque production, defining the physiological null space (Fig. 3). Because the torque generated by each muscle must be counterbalanced by activation of other muscles, those producing large torques (e.g. large moment arms and maximum isometric force) typically had low upper bounds (≤ 0.53) because of the lower torque-generating capabilities of their antagonists (Ait-Haddou et al., 2004; Jinha et al., 2006).

4. Discussion

Here, we identified the feasible ranges of individual muscle activation during endpoint force generation as a way of understanding the degree to which biomechanical redundancy allows for variability in muscle activation patterns. Feasible ranges of muscle activation were relatively unconstrained across force magnitudes in a cat hindlimb model (7 non-orthogonal DoFs, 31 muscles). Although we identified muscles that became biomechanically "necessary" at higher levels of force (e.g. nonzero lower bound), few muscles were found to be truly "necessary" at physiological force ranges. Thus, biomechanical constraints were generally insufficient to specify muscle activation levels, demonstrating that many possible muscle patterns exist that could deviate substantially from one another. In contrast, the biomechanical bounds on muscle activity in finger force generation (4 orthogonal DoFs, 7 muscles) was shown to be highly constrained, even at sub-maximal force magnitudes (Kutch and Valero-Cuevas, 2011), demonstrating differences in the biomechanical redundancy of the cat hindlimb versus the index finger.

The ubiquity of "optional" muscles in both agonist and antagonists across most force levels highlights the necessity to understand neural strategies governing selection of muscle activation patterns. The large space of functionally equivalent solutions is consistent with variations in neural and muscular activity observed across individuals in a variety of neuromotor behaviors (Klein et al., 2010; Prinz et al., 2004; Raphael et al., 2010). Moreover, "optional" muscles were never selected by typical methods that resolve biomechanical redundancy, e.g. minimizing stress (Thelen et al., 2003), or scaling patterns that produce maximal force (Valero-Cuevas, 2000), suggesting that other optimization criteria may need to be considered, such as impedance (Burdet et al., 2001), stability (Bunderson et al., 2008), fiber velocity (Walmsley et al., 1978; Prilutsky et al., 1997), metabolic energy (Alexander, 1989, 2005; Hoyt and Taylor, 1981), or more likely a combination of multiple goals in interplay (Franklin et al., 2008; Ganesh et al., 2010; Todorov, 2004). Alternatively, variations in muscle activation patterns may be due to neural constraints of activating muscles in groups (d'Avella, 2006; Hart and Giszter, 2004; Ting and Macpherson, 2005), or habitual movement patterns (de Rugy et al., 2012). One implication is that altering the biomechanical properties of a muscle, e.g. via weakening or surgery (Valero-Cuevas and Hentz, 2002; Arnold et al., 2005; Hicks et al., 2008; Correa et al., 2012), in a highly redundant system may not affect muscle activation patterns even if the force generating capabilities of muscles are altered (Scianni et al., 2009; Damiano et al., 2010).

Despite some limitations in our modeling assumptions, our estimates of feasible muscle range are likely robust and somewhat conservative. Although we specified nonzero endpoint moment, specifying a different moment values is not likely to alter our results. However, allowing a range of small endpoint moments would increase the set of redundant solutions (McKay et al., 2007), increasing the feasible range of muscle activity.

Further, individual variations in morphology of each animal compared to our generic musculoskeletal model (Burkholder and Nichols, 2004) are not expected to change the basic categorizations found. Torque-generating capabilities of muscles based on 95% optimal fiber length were only altered by -9% to $+3\%$ when physiological ranges of 80–110% optimal fiber length (Burkholder and Lieber, 2001) were used, and would not change significantly if tendon elasticity were included (Biewener et al., 1998). Finally, the activation-dependent changes in the force–length relationship (Rack and Westbury, 1969), would alter the mapping from muscle force to activation, but would only minimally affect the bounds on feasible muscle activation.

Comparing the predicted feasible muscle activation ranges to experimental data is still difficult due to differences between the model and experimental conditions. Direct comparisons of EMG to feasible limits were not possible because a reference level of muscle force was unknown (but could be estimated by maximum voluntary contraction). Further, because our technique only examines the feasible limits of a single muscle, we cannot use the predictions to identify specific multi-muscle patterns to perform a given task. The measured EMGs may not correspond exactly to the muscles or muscle groupings represented in the model. Finally, for direct comparison to our specific experimental data, we need to take into account background force for standing, which requires that the pre-existing force level be considered. For standing, this would decrease extensor force redundancy, increase flexor force redundancy, and likely have a small effect in other directions.

Nonetheless, our approach provides important insight as to the relative variability allowed for a muscle activity that is applicable to both static and dynamic tasks. In contrast to the dimension of the solution space (Bunderson et al., 2008), our approach identifies explicit constraints on muscle activation patterns. The identified bounds could be used to assess confidence of predicted muscle activity as well as possible variations when alternate cost functions or strategies are considered. The feasible muscle range also quantifies the degree to which measured muscle activity is expected to be variable or deviate from predictions. An advantage of our method is that the number of muscles that can be solved is not limited and can be applied to any high-dimensional musculoskeletal models. Our method could also be extended to analysis of dynamic tasks (Ackland et al., 2012; Thelen and Anderson, 2006; van der Krogt et al., 2012) that use methods where each time step of a movement is solved independently, e.g. inverse dynamics or static optimization (Anderson and Pandy, 2001).

Conflict of interest statement

The authors declare that they have no conflicts of interest.

Acknowledgments

References

Ackland, D.C., Lin, Y.-C., Pandy, M.G., 2012. Sensitivity of model predictions of muscle function to changes in moment arms and muscle–tendon properties: a Monte-Carlo analysis. Journal of Biomechanics 45, 1463–1471.

Ait-Haddou, R., Jinha, A., Herzog, W., Binding, P., 2004. Analysis of the force-sharing problem using an optimization model. Mathematical Biosciences 191, 111–122.

Alexander, R.M., 1989. Optimization and gaits in the locomotion of vertebrates. Physiological reviews 69, 1199–1227.

Alexander, R.M., 2005. Models and the scaling of energy costs for locomotion. Journal of Experimental Biology 208, 1645–1652.

Anderson, F.C., Pandy, M.G., 2001. Static and dynamic optimization solutions for gait are practically equivalent. Journal of Biomechanics 34, 153–161.

Arnold, A.S., Anderson, F.C., Pandy, M.G., Delp, S.L., 2005. Muscular contributions to hip and knee extension during the single limb stance phase of normal gait: a framework for investigating the causes of crouch gait. Journal of Biomechanics 38, 2181–2189.

Bernstein, N.I., 1967. The Coordination and Regulation of Movements. Pergamon Press, New York.

Biewener, A.A., Konieczynski, D.D., Baudinette, R.V., 1998. In vivo muscle force–length behavior during steady-speed hopping in tammar wallabies. Journal of Experimental Biology 201, 1681–1694.

Buchanan, T.S., Shreeve, D.A., 1996. An evaluation of optimization techniques for prediction of muscle activation patterns during isometric tasks. Journal of Biomechanical Engineering 118, 565–574.

Bunderson, N.E., Bingham, J.T., Sohn, M.H., Ting, L.H., Burkholder, T.J., 2012. Neuromechanic: a computational platform for simulation and analysis of the neural control of movement. International Journal for Numerical Methods in Biomedical Engineering 28, 1015–1027.

Bunderson, N.E., Burkholder, T.J., Ting, L.H., 2008. Reduction of neuromuscular redundancy for postural force generation using an intrinsic stability criterion. Journal of Biomechanics 41, 1537–1544.

Burdet, E., Osu, R., Franklin, D.W., Milner, T.E., Mitsuo, K., 2001. The central nervous system stabilizes unstable dynamics by learning optimal impedance. Nature 414, 446–449.

Burkholder, T.J., Lieber, R.L., 2001. Sarcomere length operating range of vertebrate muscles during movement. Journal of Experimental Biology 204, 1529–1536.

Burkholder, T.J., Nichols, T.R., 2004. Three-dimensional model of the feline hindlimb. Journal of Morphology 261, 118–129.

Correa, T.A., Schache, A.G., Graham, H.K., Baker, R., Thomason, P., Pandy, M.G., 2012. Potential of lower-limb muscles to accelerate the body during cerebral palsy gait. Gait and Posture 36, 194–200.

Crowninshield, R.D., Brand, R.A., 1981. A physiologically based criterion of muscle force prediction in locomotion. Journal of Biomechanics 14, 793–801.

d'Avella, A., 2006. Control of fast-reaching movements by muscle synergy combinations. Journal of Neuroscience 26, 7791–7810.

Damiano, D.L., Arnold, A.S., Steele, K.M., Delp, S.L., 2010. Can strength training predictably improve gait kinematics? A pilot study on the effects of hip and knee extensor strengthening on lower-extremity alignment in cerebral palsy. Physical Therapy 90, 269–279.

de Rugy, A., Loeb, G.E., Carroll, T.J., 2012. Muscle coordination is habitual rather than optimal. Journal of Neuroscience 32, 7384–7391.

Erdemir, A., McLean, S., Herzog, W., van den Bogert, A.J., 2007. Model-based estimation of muscle forces exerted during movements. Clinical Biomechanics 22, 131–154.

Franklin, D.W., Burdet, E., Peng Tee, K., Osu, R., Chew, C.M., Milner, T.E., Kawato, M., 2008. CNS learns stable, accurate, and efficient movements using a simple algorithm. Journal of Neuroscience 28, 11165–11173.

Ganesh, G., Haruno, M., Kawato, M., Burdet, E., 2010. Motor memory and local minimization of error and effort, not global optimization, determine motor behavior. Journal of Neurophysiology 104, 382–390.

Hart, C.B., Giszter, S.F., 2004. Modular premotor drives and unit bursts as primitives for frog motor behaviors. Journal of Neuroscience 24, 5269–5282.

Herzog, W., Leonard, T.R., 1991. Validation of optimization models that estimate the force exerted by synergistic muscles. Journal of Biomechanics 24, 31–39.

Hicks, J.L., Schwartz, M.H., Arnold, A.S., Delp, S.L., 2008. Crouched postures reduce the capacity of muscles to extend the hip and knee during the single-limb stance phase of gait. Journal of Biomechanics 41, 960–967.

Horak, F.B., Nashner, L.M., 1986. Central programming of postural movements: adaptation to altered support–surface configurations. Journal of Neurophysiology 55, 1369–1381.

Hoyt, D.F., Taylor, C.R., 1981. Gait and the energetics of locomotion in horses. Nature 292, 239–240.

Jacobs, R., Macpherson, J.M., 1996. Two functional muscle groupings duting postural equilibrium tasks in standing cats. Journal of Neurophysiology 76, 2402–2411.

Jinha, A., Ait-Haddou, R., Herzog, W., 2006. Predictions of co-contraction depend critically on degrees-of-freedom in the musculoskeletal model. Journal of Biomechanics 39, 1145–1152.

Klein, D.A., Patino, A., Tresch, M.C., 2010. Flexibility of motor pattern generation across stimulation conditions by the neonatal rat spinal cord. Journal of Neurophysiology 103, 1580–1590.

Kutch, J.J., Valero-Cuevas, F.J., 2011. Muscle redundancy does not imply robustness to muscle dysfunction. Journal of Biomechanics 44, 1264–1270.

McKay, J.L., Burkholder, T.J., Ting, L.H., 2007. Biomechanical capabilities influence postural control strategies in the cat hindlimb. Journal of Biomechanics 40, 2254–2260.

McKay, J.L., Ting, L.H., 2008. Functional muscle synergies constrain force production during postural tasks. Journal of Biomechanics 41, 299–306.

Prilutsky, B.I., Herzog, W., Allinger, T.L., 1997. Forces of individual cat ankle extensor muscles during locomotion predicted using static optimization. Journal of Biomechanics 30, 1025–1033.

Prinz, A.A., Bucher, D., Marder, E., 2004. Similar network activity from disparate circuit parameters. Nature Neuroscience 7, 1345–1352.

Rack, P.M., Westbury, D.R., 1969. The effects of length and stimulus rate on tension in the isometric cat soleus muscle. Journal of Physiology 204, 443–460.

Raphael, G., Tsianos, G.A., Loeb, G.E., 2010. Spinal-like regulator facilitates control of a two-degree-of-freedom wrist. Journal of Neuroscience 30, 9431–9444.

Roy, R.R., Kim, J.A., Monti, R.J., Zhong, H., Edgerton, V.R., 1997. Architectural and histochemical properties of cat hip 'cuff' muscles. Acta Anatomica 159, 136–146.

Sacks, R.D., Roy, R.R., 1982. Architecture of the hind limb muscles of cats: functional significance. Journal of Morphology 173, 185–195.

Scianni, A., Butler, J.M., Ada, L., Teixeira-Salmela, L.F., 2009. Muscle strengthening is not effective in children and adolescents with cerebral palsy: a systematic review. Australian Journal of Physiotherapy 55, 81–87.

Thelen, D.G., Anderson, F.C., 2006. Using computed muscle control to generate forward dynamic simulations of human walking from experimental data. Journal of Biomechanics 39, 1107–1115.

Thelen, D.G., Anderson, F.C., Delp, S.L., 2003. Generating dynamic simulations of movement using computed muscle control. Journal of Biomechanics 36, 321–328.

Ting, L.H., Macpherson, J.M., 2004. Ratio of shear to load ground-reaction force may underlie the directional tuning of the automatic postural response to rotation and translation. Journal of Neurophysiology 92, 808–823.

Ting, L.H., Macpherson, J.M., 2005. A limited set of muscle synergies for force control during a postural task. Journal of Neurophysiology 93, 609–613.

Todorov, E., 2004. Optimality principles in sensorimotor control. Nature Neuroscience 7, 907–915.

Torres-Oviedo, G., Macpherson, J.M., Ting, L.H., 2006. Muscle synergy organization is robust across a variety of postural perturbations. Journal of Neurophysiology 96, 1530–1546.

Torres-Oviedo, G., Ting, L.H., 2007. Muscle synergies characterizing human postural responses. Journal of Neurophysiology 98, 2144–2156.

Valero-Cuevas, F.J., 2000. Predictive modulation of muscle coordination pattern magnitude scales fingertip force magnitude over the voluntary range. Journal of Neurophysiology 83, 1469–1479.

Valero-Cuevas, F.J., Hentz, V.R., 2002. Releasing the A3 pulley and leaving flexor superficialis intact increases pinch force following the Zancolli lasso procedures to prevent claw deformity in the intrinsic palsied finger. Journal of Orthopaedic Research 20, 902–909.

van der Krogt, M.M., Delp, S.L., Schwartz, M.H., 2012. How robust is human gait to muscle weakness? Gait and Posture 36, 113–119.

Walmsley, B., Hodgson, J.A., Burke, R.E., 1978. Forces produced by medial gastrocnemius and soleus muscles during locomotion in freely moving cats. Journal of Neurophysiology 41, 1203–1216.

Zajac, F.E., 1989. Muscle and tendon: properties, models, scaling, and application to biomechanics and motor control. Critical Reviews in Biomedical Engineering 17, 359–411.